Investigation of RF-Sputtered Tin Sulfide Thin Films with *in situ* Heating for Photovoltaic Applications

Rona E. Banai, Hyeonseok Lee, Nicholas J. Tanen, Rafael E. Urena,
Jacob J. Cordell, Mark W. Horn, Jeffrey R. S. Brownson

The Pennsylvania State University, University Park, PA 16802, USA

***Abstract*—Tin (II) Monosulfide (SnS) is of increasing interest to researchers due to its near-optimal optoelectronic properties for photovoltaic devices. In this work, we take a new approach using a Tin (IV) Disulfide target to sputter SnS thin films. Sulfur-rich SnS thin films are produced via *in situ* heating of the substrate. Experimentation with substrate heating has yielded two unique crystal structures, depending on constant or "pulsed" heating. Standardless Electron Dispersive Spectroscopy measurements indicate that the films are nearly 1:1 Sn:S ratio. Films with low resistivity (<100 Ω-cm) were produced via this method. These results are promising for improving SnS-based photovoltaic device performance.**

***Index Terms*—semiconductor materials, SnS, SnS_2, sputtering, thin films, tin compounds, X-ray diffraction.**

I. Introduction

Tin (II) Monosulfide (SnS) has become an interesting alternative material for thin film photovoltaics (PV). The optoelectronic properties indicate that SnS is a suitable material for PV. Its high absorption coefficient above 10^4 cm^{-1} [1] and band gap near 1.3 eV [2] are well matched with the solar spectrum. SnS also has a carrier concentration greater than 10^{15} cm^{-3} [3], and potential to be both n-type and p-type [4], [5]. With recent success in achieving 4% efficiency, SnS-based devices demonstrated their potential. [6] Improvement to the SnS layer is still crucial to reaching higher device efficiencies.

While a variety of deposition methods have been attempted for SnS thin films, a large variety in results is seen in the literature. Previous work demonstrated several deposition methods of SnS including electrochemical deposition [7], [8], sulfurization of tin thin films [9], thermal evaporation [1], sputtering [10], [11], atomic layer deposition [12], and pulsed chemical vapor deposition [13]. Sputter deposition offers the ability to fine-tune deposition conditions and tailor the properties of thin films. Through precise control of chamber pressure, radio frequency (RF) power, substrate temperature and target-to-substrate throw distance, SnS thin films can be deposited for a range of crystallinity and morphology. [11] The ability to tune the quality of thin films is necessary to understand and optimize the properties of SnS. Previous results reported established a baseline for producing SnS layers via radio-frequency (RF) sputtering of a SnS target. [11], [14], [15] These studies focused on optical properties, phases, and crystallographic orientation of SnS thin films. Electronic properties were difficult to characterize for these films due to large contact resistance; thus, a new avenue for sputtering SnS was pursued by using a tin (IV) disulfide (SnS_2) target with *in situ* heating of the substrate.

One major issue with deposition SnS thin films via thermal methods is the high volatility of sulfur leading to sulfur-deficient thin films. [1], [10], [16] Significant challenges in producing sulfur-rich SnS thin films suggest that most SnS-based devices could have this issue. While sulfur deficient films are p-type, they are likely to contain unwanted defects, which can significantly impact device performance. Starting with a source material that has higher sulfur content can reduce this problem. For sputter deposition, a SnS_2 target can add the needed excess sulfur to produce stoichiometric SnS thin films. In this study, a SnS_2 target is used during sputter deposition, with *in situ* heating for improved SnS film quality, and to assist in vaporizing excess sulfur. Substrate temperature and method of heating were investigated in this study. To the authors' knowledge, this is the first report of *in situ* substrate heating while RF-sputtering a SnS_2 target.

II. Methods and Materials

Tin sulfide thin films are deposited in a radio frequency (RF) magnetron sputtering system in a downward vertical geometry at room temperature. A 3" diameter target used was tin disulfide of 99.999% purity (LTS Research Laboratories, Inc.). Films were co-deposited on silicon nitride coated silicon wafers and glass microscope slides. Target-to-substrate throw distance was 12 cm. Base pressures below 2×10^6 Torr were achieved using a turbomolecular pump and measured with an ion gauge. Argon plasmas were ignited at 60 to 70 mTorr with the shutter closed and then the shutter was opened for depositions at pressures of 40 mTorr. Chamber pressure was measured with a convectron gauge. RF-power was 115 W for all films in this study.

A ceramic heater was used for substrate heating. Substrate temperatures ranged from 130-300°C. In this study, four samples were heated constantly during the deposition, while the remaining four were not. Power to the ceramic heater was "pulsed" by supplying power for 2 minutes every 4

TABLE I
LIST OF SAMPLES, CORRESPONDING DEPOSITION CONDITIONS, AND NUMERICAL RESULTS

Sample	Target Power (W)	Pressure (mTorr)	Temperature (°C) Initial	Final	Heat Method	Thickness (Å)	Sn:S Ratio	Resistivity (Ω-cm)	Contact Resistance (Ω)
CH200	115	40	206	195	Constant	4270	1:1.34	4.7	500
CH180	115	40	164	200	Constant	6950	1:1.41	21.2	6,100
CH140	115	40	128	148	Constant	1710	1:1.37	45.8	–
CH230	115	40	256	212	Constant	4070	1:1.37	79.0	–
PH150	115	40	162	144	Pulsed	3360	1:1.43	–	$> 1.3 \times 10^{10}$
PH120	115	40	116	125	Pulsed	3500	1:1.44	–	$> 1.9 \times 10^{9}$
PH190	115	40	214	173	Pulsed	5950	1:1.47	9.7	7,900
PH230	115	40	261	198	Pulsed	6540	1:1.39	16.1	2,000

minutes for the remaining samples. All depositions lasted 20 minutes. The purpose of pulsed heating was to maintain a more constant temperature during the deposition. In this set up, temperature was measured at start and finish of deposition, but not during due to interference between the RF power and the thermocouple. Table I summarizes deposition conditions of the samples examined in this study.

SnS films were characterized by several methods to determine thickness, morphology, crystallinity and resistivity. Film thickness was determined using a Tencor Profilometer. Surface morphology of the SnS films was assessed using the ZeissSMT1530, high-resolution Field Emission Scanning Electron Microscope (FESEM). Cross-sectional SEM was used to check thickness of films where thickness was not available by profilometry. SnS phase analysis and structural properties were measured using glancing incidence X-ray diffraction (GIXRD) at an incident angle of 1° and detected from 10° to 70° (PANalytical XPert Pro MPD). [11]

Composition was determined via electron dispersive spectroscopy (EDS) using an Oxford detector on a FEI Nova NanoSEM 630 FESEM. EDS measurements were standardized using a single crystal SnS sample. An accelerating voltage of 20 keV was used for both the standard and thin film samples. Validity of these measurements was checked with thin films also measured using Rutherford Backscattering Spectroscopy. Values matched within 1% nominally across the two methods.

Resistivity was determined via transmission line method (TLM). TLM contacts were made by sputtering 100 nm of titanium on the surface of the films. TLM patterns were 6 mm long, with five lines spaced 0.2, 0.3, 0.5, and 0.7 cm apart. Resistivity values were determined from top contacts only.

III. RESULTS AND DISCUSSION

Table I shows the summary of samples analyzed in this study including deposition conditions, film thickness, Sn:S ratio and resistivity. A uniform temperature was difficult to maintain during the deposition. This difficulty was expected to affect film properties. Initial and final temperatures were recorded for these depositions. The temperature differential for depositions ranged from 11°C to 63°C. The impact of a larger temperature differential appears to depend on the positive or negative change in temperature, which is seen in XRD patterns. Temperature changes during the deposition were not independent of plasma processes. Without the plasma, the heater temperature differential sometimes results in higher final temperatures after 20 minutes relative to depositions. This observation suggests that the depositing film absorbs a significant amount of energy from the heater, acting as a heat sink. Therefore, the atoms on the substrate are likely to absorb much of the heat supplied. This directly affects the adatom mobility, growth mode and as a result, the film properties.

EDS measurements suggest that all films have a thin oxide surface layer. Composition of all films was fairly close, to a Sn:S ratio of 2:3. Composition does not trend with substrate temperature for either constant or pulsed heating. This composition suggests that the films may be primarily Sn_2S_3 or a near-even mixture of SnS and SnS_2. XRD patterns do not match the Sn_2S_3 pattern diffraction files. XRD patterns of films do not distinctly match both SnS and SnS_2 phases; thus phase identification cannot be reported with confidence.

XRD patterns shown in Fig. 1a do not follow a systematic trend for peak intensity with respect to substrate temperature. The drastic change in temperature for sample CH230 could affect the resulting crystallographic orientation. The samples are arranged from top to bottom with decreasing intensity of the 15° peak. A secondary effect is evident at the peak near 31°, which increases in intensity as the 15° peak decreases. Additionally, the 15° peak is much narrower than the 31° peak for all films. This suggests that crystallites matching each of these peaks are of different size, or that multiple orientations are hidden in the single peak. This is a likely possibility as herzenbergite has several crystal orientations near 31°. For sample CH230, the phase matching the 31° peak dominates the film, but the crystallites are likely to be smaller than the other films. The evolution of these peaks might be expected to trend with substrate temperature; however, the trend does not align with substrate temperature and must be a result of a secondary effect. The 15° peak is suppressed in pulsed heated films which suggests that the growth mode is different for these films.

The peak near 15° for the films made with constant heating indicates that the films have a crystal structure with larger lattice spacing. Using Bragg's Law, the lattice spacing for those films was calculated as 5.99 Å. Sample CH140 has two large peaks of similar intensity, which suggests that crystallites in the film are nearly mixed orientation, and mixed phases.

Pulsing the voltage to the heater drastically affects the x-ray diffraction pattern, as seen in Fig. 1b. Pulsed heating at higher temperatures produced a dominant herzenbergite phase. XRD showed no or minimal peaks for pulsed heated depositions

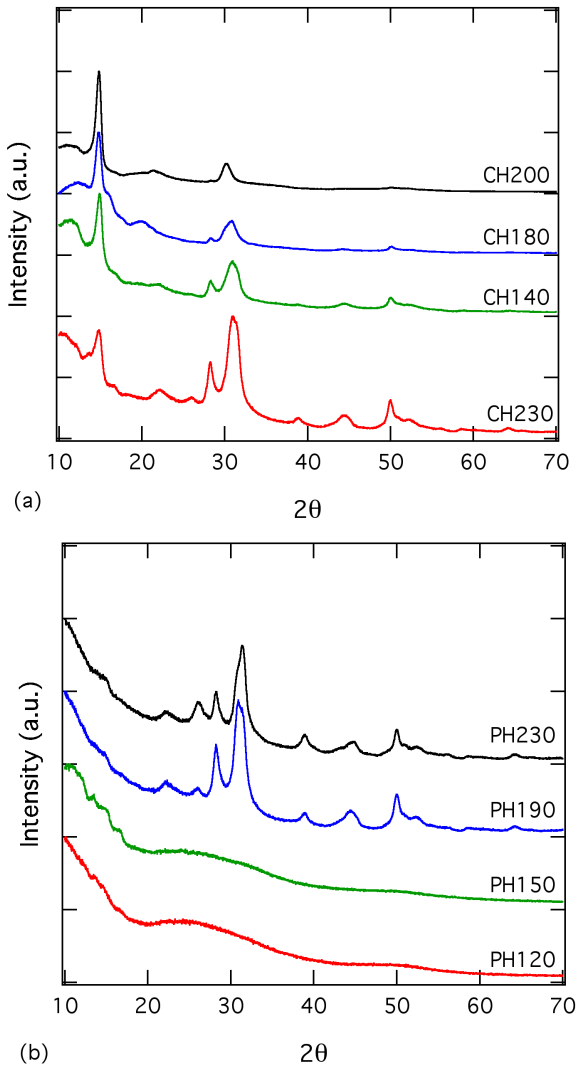

Fig. 1. X-ray diffraction patterns of samples listed in Table I. (a) Samples produced with constant heat. (b) Samples produced with pulsed heat.

at lower temperatures. Substrate temperatures greater than 160°C seem necessary to induce crystallinity for pulsed heated depositions, whereas constant heating at temperatures greater than 140°C was sufficient for constant heating. The large temperature drop during the deposition for samples PH190 and PH230 also occured for sample CH230. These three samples also have similar XRD patterns, excluding the 15° peak in sample CH230. The result suggests that the induced phase seen in XRD patterns is caused by the large temperature drop during deposition.

Fig. 2 shows the high temperature films primarily produced a leaf-like morphology with sample CH200 as the exception. Sample CH200 has small crystallites, but exhibited very low resistivty as listed in Table I. The high density of the crystallites is good for electronic properties. The crystallites in sample CH200 are larger than those seen in samples PH120 and PH150. Fig. 2b shows that samples PH150 and PH120 are nanocrystalline, which is verified by the lack of peaks found in their XRD patterns as shown in Fig. 1b. While crystallographic orientation of these films is very different for all films, both pulsed heated and constantly heated film crystals display a reticulated leaf-like habit. “Leaves” in sample CH230 are spaced far enough apart to see that below them there are smaller round crystallites similar to sample CH200, which does not exhibit the leaf-like morphology. It is unclear if this feature is unique to samples CH230 and CH200, but the results suggest that small crystallites could like underneath any films with leaf-like morphology.

The leaf-like morphology has been seen with other deposition methods, including hot wall deposition [17], [18] and electochemical deposition [7], [19]. It is surprising that this morphology is found because the growth conditions vary considerably with respect to thermodynamic equilibrium. The morphology indicates that the primary growth mode is parallel to the layers. Whereas hot wall deposition occurs at thermodynamic equilibrium, electrochemical deposition and sputtering do not. In addition, the leaf-like morphology did not occur while sputtering a SnS target. [11], [15] The presence of excess

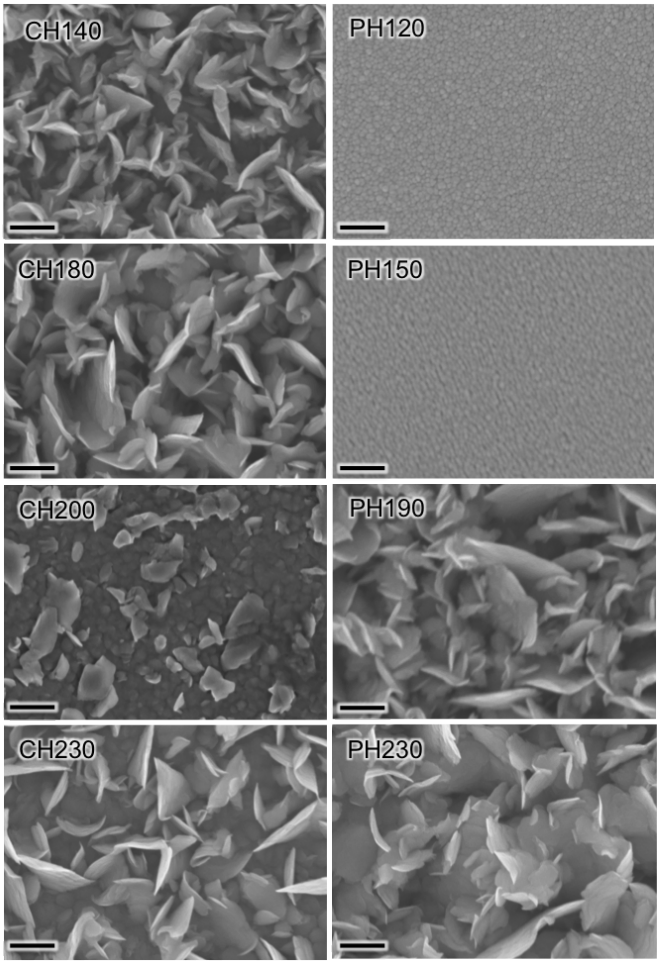

Fig. 2. Scanning electron microscopy images of all samples listed in Table I. Scale bars are equal and set to 200 nm.

sulfur induced a similar growth mode similar to those other deposition methods. The growth rate is likely to be very rapid in the plane of the "leaves". The nature of the crystal structure also allows for growth to occur perpendicular from the plane. Deposition rates for samples made using the SnS target were mostly 25% faster for the SnS_2 target with identical conditions. Excess sulfur could induce faster deposition rates because the electric field of the plasma encourages acceleration of negative ions towards the substrate.

The leaf-like morphology makes them prone to scratching and "smoothing" of the surface. The soft surface is likely non-optimal for forming ohmic contacts. Because sputtering results in high-energy bombardment of atoms on the surface, Ti atoms landing on soft SnS_x could change the state of the surface, affecting the nature of the contact between SnS_x and Ti. Fig. 3 shows an example of TLM results for samples CH200 and PH190. Sample CH200 made very good ohmic contact with Ti as seen from the perfect linearity of the Current voltage

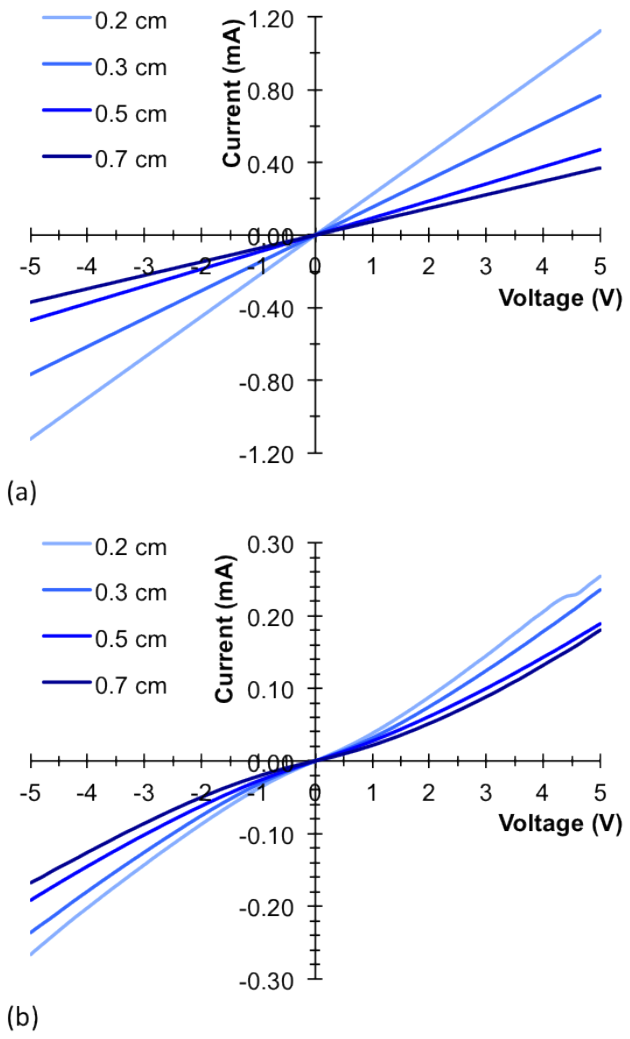

Fig. 3. Current-Voltage curves from TLM patterns for samples CH200 (a) and PH190 (b).

(I-V) curves. SEM of this sample showed that it did not have leaf-like morphology. I-V curves for TLM measurements of other films were slightly non-linear for some of these films, which could be due to an oxide layer, or the soft surface due to their morphology. Fig. 3b shows an example of imperfect I-V curves for sample PH190.

Ti has a work function of 4.33 eV [20], while SnS, Sn_2S_3, and SnS_2 have an electron affinities of 4.70, 5.35 and 7.30 eV respectively [21]. If these films are indeed p-type, the band alignment of Ti with any of these phases of tin sulfide indicates that the contacts with these films should not be ohmic with these thin films. At this stage phase content has not been verified for these films, so these calculated electron affinities may not be relevant. Regardless, the high contact resistance necessitates further investigation of these films will be necessary in order to obtain accurate resistivities for deposited films.

TLM measurements with Ti top contacts were done for all samples. Due to high contact resistance, it was not possible to determine resistivity via this method for samples PH150 and PH120. Because these films are nanocrystalline, it is expected that they have poor electrical characteristics. Their pulsed heated nature apparently resulted in temperatures too low to allow growth of crystallites. On the other hand, sample CH140 was grown with constant heat at a similar temperature range, and showed crystallite growth. Sample CH140 has reasonable resistivity, comparable to the other films, despite a low substrate temperature during growth.

Table I lists the resistivities found via TLM measurements. While XRD patterns indicate that the films are very different in phase, morphology and resistivity information suggest that the films can have similar properties. Excluding the nanocrystalline films, these films have low resistivities. Pulsed heated samples at sufficiently high temperatures also have similar resistivities, XRD patterns and morphology. For these films, the large temperature differential during deposition did not result in poor conductivity. The change in substrate temperature possibly affected the transition from nucleation to growth mode changed to result in better properties.

The results for constant heating are different from those for pulsed heating. Samples CH180 and CH230 both had large temperature differentials, but resistivities differ significantly. Better film quality was achieved for pulsed heating at the higher temperatures above 190°C or for constant heating from 180 to 200°C. Individual TLM measurements for samples CH140, CH180, and CH230 showed good ohmic contacts with Ti. However, resistance values derived from measurements were non-linear for these samples. Therefore, the resistivities for these samples have a large range of error. Both a surface oxide layer and the soft morphology could cause the variability in measurements for these samples.

IV. Conclusion

A new avenue for producing SnS was achieved by sputtering a SnS_2 target with *in situ* heating of the substrate. The excess sulfur from the target results in sulfur rich films with a Sn:S

ratio near 2:3. Substrate temperature did not correlate to film composition, but higher temperatures are expected to decrease the sulfur content of films. Excess sulfur also allows for future post-deposition annealing to be utilized to improve film quality and could produce stoichiometric SnS. Experiments of annealed thin films produced from the SnS_2 target will be described in future work.

The two *in situ* heating methods studied showed the high sensitivity of film properties to processing method. Temperature variation during the deposition significantly impacted XRD patterns. A large drop in temperature resulted in higher intensity of peaks matching Herzenbergite SnS phase. Constant heating with lower temperature differentials resulted in a large peak near 15°, which matches a lattice spacing of 5.99 Å. Further analysis of the phases present in films will be studied in future work.

While morphology seen in SEM micrographs showed small crystallites, or leaf-like structure, TLM measurements showed the films to have low resistivities. The resistivities were significantly lower than films sputtered from a SnS target. The excess sulfur from the SnS_2 target was found to improve electronic properties of SnS_x thin films. The results are promising for producing high quality films for SnS-based PV devices.

ACKNOWLEDGMENT

Many of the characterizations done for this paper were done in the Materials Characterization Laboratory at Penn State. The authors appreciate the assistance received at these facilities, especially that of Nichole Wonderling and Julie Anderson.

REFERENCES

[1] M. Devika, N. Koteeswara Reddy, K. Ramesh, R. Ganesan, K. R. Gunasekhar, E. S. R. Gopal, and K. T. Ramakrishna Reddy, "Thickness effect on the physical properties of evaporated SnS films," *Journal of the Electrochemical Society*, vol. 154, no. 2, pp. H67–H73, Dec 2007.

[2] A. R. H. F. Ettema, R. A. de Groot, and C. Haas, "Electronic structure of SnS deduced from photoelectron spectra and band-structure calculations," *Physical Review B*, vol. 46, no. 12, pp. 7363–7373, Sept 1992.

[3] K. T. Ramakrishna Reddy, N. K. Reddy, and R. W. Miles, "Photovoltaic properties of SnS based solar cells," *Solar Energy Materials and Solar Cells*, vol. 90, no. 18-19, pp. 3041–3046, Nov 2006.

[4] P. A. Nwofe, K. T. Ramakrishna Reddy, and R. W. Miles, "Type conversion of p-SnS to n-SnS using a $SnCl_4/CH_3OH$ heat treatment," *Conference Record of the 39th IEEE Photovoltaics Specialists Conference*, pp. 2518 – 2523, 2013.

[5] C. C. Huang, Y. J. Lin, C. Y. Chuang, C. J. Liu, and Y. W. Yang, "Conduction-type control of SnS_x films prepared by the sol–gel method for different sulfur contents," *Journal of Alloys and Compounds*, vol. 553, pp. 208–211, 2013.

[6] K. Hartman, R. Jaramillo, V. Steinmann, R. Chakraborty, H. H. Park, R. G. Gordon, and T. Buonassisi, "Annealing SnS thin films in controlled sulfur environments for improved photovoltaic performance," in *2013 MRS Fall Meeting*. MRS, 2013.

[7] J. R. S. Brownson, C. Georges, and C. Lévy-Clément, "Synthesis of a δ-SnS polymorph by electrodeposition," *Chemistry of Materials*, vol. 18, pp. 6397–6402, Dec 2006.

[8] S. Cheng, G. Chen, Y. Chen, and C. Huang, "Effect of deposition potential and bath temperature on the electrodeposition of SnS film," *Optical Materials*, vol. 29, pp. 439–444, Feb 2006.

[9] K. T. Ramakrishna Reddy, P. Purandhara Reddy, P. K. Datta, and R. W. Miles, "Formation of polycrystalline SnS layers by a two-step process," *Thin Solid Films*, vol. 403-404, pp. 116–119, 2002.

[10] K. Hartman, J. L. Johnson, M. I. Bertoni, D. Recht, M. Aziz, M. A. Scarpulla, and T. Buonassisi, "SnS thin-films by RF sputtering at room temperature," *Thin Solid Films*, vol. 519, no. 7421–7424, Dec 2010.

[11] R. E. Banai, H. Lee, M. A. Motyka, R. Chandrasekharan, N. J. Podraza, J. R. S. Brownson, and M. W. Horn, "Optical properties of sputtered SnS thin films for photovoltaic absorbers," *IEEE Journal of Photovoltaics*, vol. 3, no. 3, pp. 1084–1089, Jul 2013.

[12] P. Sinsermsuksakul, J. Heo, W. Noh, A. S. Hock, and R. G. Gordon, "Atomic layer deposition of tin monosulfide thin films," *Advanced Energy Materials*, vol. 1, pp. 1116–1125, 2011.

[13] P. Sinsermsuksakul, K. Hartman, S. B. Kim, J. Heo, L. Sun, H. H. Park, R. Chakraborty, T. Buonassisi, and R. G. Gordon, "Enhancing the efficiency of SnS solar cells via band-offset engineering with a zinc oxysulfide buffer layer," *Applied Physics Letters*, vol. 102, p. 053901, Feb 2013.

[14] R. E. Banai, H. Lee, M. Lewinsohn, M. A. Motyka, R. Chandrasakharan, N. J. Podraza, J. R. S. Brownson, and M. W. Horn, "Investigation of the absorption properties of sputtered SnS thin films," *Conference Record of the 38th IEEE Photovoltaics Specialists Conference*, pp. 164–169, Jun 2012.

[15] R. E. Banai, H. Lee, S. Zlotnikov, J. R. S. Brownson, and M. W. Horn, "Phase identification of RF-sputtered SnS thin films using rietveld analysis of X-ray diffraction patterns," *Conference Record of the 39th IEEE Photovoltaics Specialsts Conference*, pp. 2562 – 2566, Jun 2013.

[16] M. Devika, N. K. Reddy, D. S. Reddy, Q. Ahsunlhaq, K. Ramesh, E. S. R. Gopal, K. R. Gunasekhar, and Y. B. Hahn, "Synthesis and characterization of nanocrystalline films grown by thermal evaporation technique," *Journal of the Electrochemical Society*, vol. 155, no. 2, pp. H130–H135, 2008.

[17] S. A. Bashkirov, V. F. Gremenok, V. A. Ivanov, and V. V. Shevtsova, "Microstructure and electrical properties of SnS thin films," *Surface Physics and Thin Films*, vol. 54, pp. 2497–2502, Apr 2012.

[18] S. P. Zimin, E. S. Gorlachev, I. I. Amirov, V. V. Naumov, G. A. Dubov, V. F. Gremenok, and S. A. Bashkirov, "Investigations of nanocrystalline SnS films' surface morphology modification during inductively coupled argon plasma sputtering," *Semiconductor Science and Technology*, vol. 29, p. 015009 015009, 2014.

[19] J. R. S. Brownson, C. Georges, G. Larramona, A. Jacob, B. Delatouche, and C. Lévy-Clément, "Chemistry of tin monosulfide (δ-SnS) electrodeposition: Effects of pH and temperature with tartaric acid," *Journal of the Electrochemical Society*, vol. 155, pp. D40–46, Jan 2008.

[20] E. H. Rhoderick and R. H. Williams, *Metal-Semiconductor Contacts*, second edition ed. New York: Oxford University Press, 1988.

[21] L. A. Burton, D. Colombra, R. D. Abellon, F. C. Grozema, L. M. Peter, T. J. Savenije, G. Dennler, and A. Walsh, "Synthesis, characterization, and electronic structure of single- crystal SnS, Sn_2S_3, and SnS_2," *Chemistry of Materials*, vol. 25, pp. 4908–4916, 2013.